Available online at www.sciencedirect.com
SCIENCE DIRECT®

PALAEO

Palaeogeography, Palaeoclimatology, Palaeoecology 234 (2006) 277–286

www.elsevier.com/locate/palaeo

Late Quaternary glacial history in the Encierro Valley, northern Chile (29°S), deduced from ^{10}Be surface exposure dating

Roland Zech [a,*], Christoph Kull [a,b], Heinz Veit [a]

[a] *Geographical Institute, University of Bern, Hallerstr. 12, 3012 Bern, Switzerland*
[b] *PAGES IPO, Sulgeneckstrasse 38, 3007 Bern, Switzerland*

Received 4 May 2005; received in revised form 12 October 2005; accepted 13 October 2005

Abstract

The Late Pleistocene glacial and climate history in the dry Central Andes is not well known so far, mainly because of the lack of suitable material for radiocarbon dating. In order to establish a glacial chronology, we applied surface exposure dating, using in-situ produced cosmogenic ^{10}Be, for 11 boulders from moraines in the Encierro Valley (29°S), northern Chile. We discuss sample-specific effects (topographic shielding, sample geometry, rock surface erosion, inheritance and post-depositional geomorphological instability) and systematic uncertainties (production rate of ^{10}Be, latitude and altitude scaling). Minor glacial advances probably occurred around 11.6 ± 1.2 ka BP, whereas major advances are recorded at 14.0 ± 1.4 ka BP and eventually at 24.1 ± 2.4 ka BP.

This may indicate synchrony of some Late Pleistocene glacial advances south and north of the so-called Arid Diagonal (~25°S). Increased precipitation plays a dominant role for the observed Late Pleistocene glacial advances. In the absence of further glacial chronologies south and north of the research area, it remains difficult to disentangle the influence of the complex and in space and time variable westerlies and the tropical summer precipitation regime.

Keywords: Cosmogenic nuclides; Exposure dating; Chile; Arid diagonal; Quaternary; Glaciation

1. Introduction

The arid Central Andes in South America are a key area for the study of Late Quaternary climate changes because they mark a transition zone between tropical and extra-tropical circulation systems (Fig. 1). Any changes in large-scale atmospheric circulation patterns should therefore be recorded in lacustrine, fluvial and glacial deposits. The palaeo-environmental reconstruction at key sites, like, e.g. along the "Arid Diagonal" that crosses the Andes at 25–27°S, improves our understanding of the climate system. Besides, the expected impact of global changes in South America can only be recognised and fully understood through the reliable knowledge and interpretation of global changes in the past (IPCC, 2001).

Knowledge of Late Pleistocene climate changes in the Central Andes is still limited (Garleff and Stingl, 1991, 1998; Harrison, 2004; Heine, 2004; Mark et al., 2004). This is mainly due to the lack of suitable organic material for radiocarbon dating. The climate in the Central Andes is very arid so that conditions for organic matter production and preservation are extremely unfavourable. Due to the aridity, no glaciers exist today between 18°S (Vulcan Sajama) and 27°S (Cerro Tres Cruzes), even despite of elevations up to 6700 m

* Corresponding author. Tel.: +41 31 6318019; fax: +41 31 6318511.
E-mail address: Roland.Zech@giub.unibe.ch (R. Zech).

0031-0182/$ - see front matter © 2005 Elsevier B.V. All rights reserved.
doi:10.1016/j.palaeo.2005.10.011

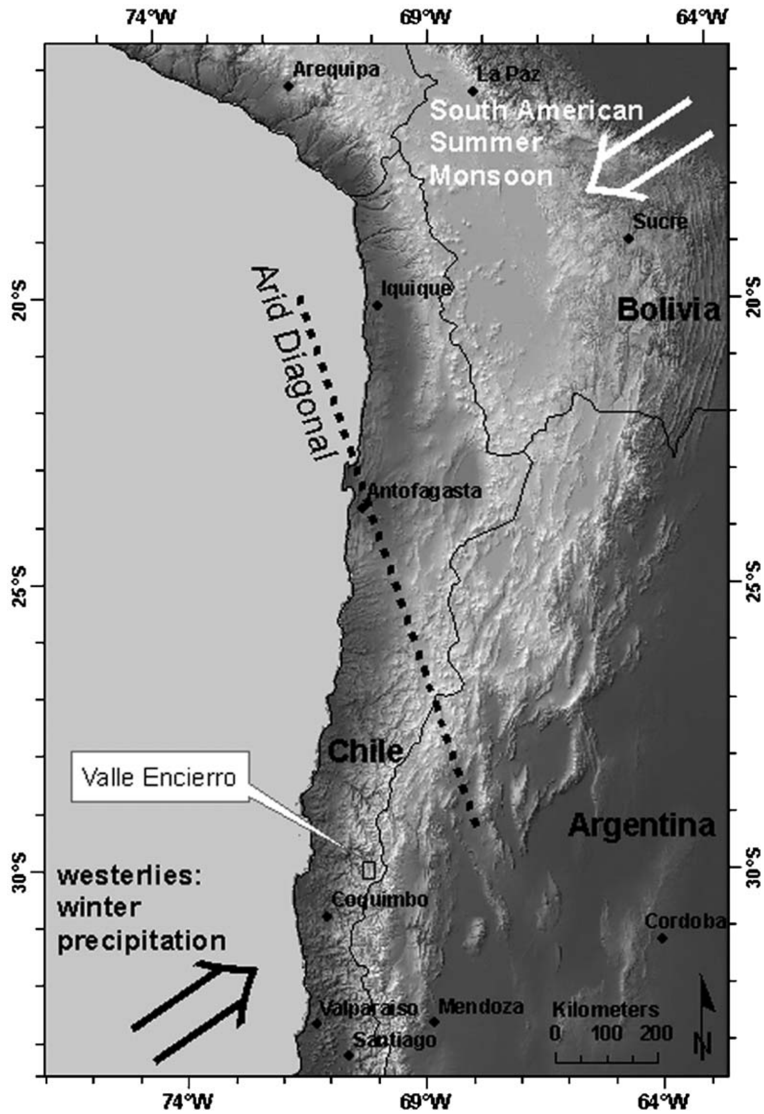

Fig. 1. Location of the research area and atmospheric circulation patterns providing moisture to the arid Central Andes.

(Grosjean et al., 1998; Veit, 2000). This phenomena, known as 'thermal readiness' (Messerli, 1973), implies that glacier growth is not limited by temperature, but by insufficient precipitation. Large moraines north and south of the Arid Diagonal (Jenny and Kammer, 1996) document at least one Late Pleistocene phase of substantially increased precipitation.

North of the Arid Diagonal, late-glacial transgression phases (Tauca) are well documented (Baker et al., 2001; Chepstow-Lusty et al., 2005; Fritz et al., 2004; Grosjean et al., 1995; Sylvestre et al., 1999) and have been confirmed to be synchronous with last maximum glacial advances (Clapperton et al., 1997; Clayton and Clapperton, 1997). Maximum glacial advances did thus not occur during the temperature minimum of the global last glacial maximum (LGM) at 18–20 ka before present (BP). Instead, the glacial and lacustrine history was mainly controlled by increased monsoonal moisture advection from the Atlantic and the Amazon Basin (Ammann et al., 2001; Hastenrath and Kutzbach, 1985; Kull and Grosjean, 1998).

Evidence for a humid late-glacial phase disappears south of 25°S (Geyh et al., 1999; Grosjean et al., 1995). Timing and precipitation source during the maximum glacier expansion south of the Arid Diagonal are not yet known. Today, most precipitation south of the Arid Diagonal is derived from extra-tropical winter precipitation with Pacific moisture related to cyclone activity (Vuille and Ammann, 1997). Based on a glacier climate model, which was applied north (Kull, 1999; Kull and Grosjean, 2000; Kull et al., 2003) and south (Kull et al., 2002) of the Arid Diagonal, it was suggested that different climatic conditions in the respective study areas, especially temperature, point to different timing of the most dominant glacial advance. Glaciers in the south might have reached their maximum extent under full glacial climate conditions around the LGM, i.e. synchronous with dated glacial advances in Central and Southern Chile (Denton et al., 1999; Espizua, 1999; Heusser et al., 1999; Lowell et al., 1995). The necessary increase in annual precipitation at ~30°S (Kull et al., 2002) during full glacial times is consistent with modelling studies (Caviedes, 1990; Wyrwoll et al., 2000) and with findings from coastal sediments (Stuut and Lamy, 2004).

Ammann et al. (2001) emphasised the lack of glacial deposits at latitudes from 25°S to 27°S. It is not possible to confidently correlate the most prominent lateglacial stage north of the Arid Diagonal with the most prominent, hitherto undated Late Pleistocene glacial advance south of the Arid Diagonal. In the absence of absolute dates, timing and extent of glacial advances remains speculative there.

In this paper, we present the first results of a palaeoecological study that tries to contribute to the reconstruction of the Late Pleistocene climate history along a transect from the Bolivian Andes in the north to the Patagonian Andes in the south. One of the main objectives is the direct numerical dating of moraines using ^{10}Be surface exposure dating. Here, we discuss exposure ages of 11 boulders from moraines in the Encierro Valley just south of the Arid Diagonal (29°S), (i) with respect to their stratigraphical position and (ii) in terms of the uncertainties concerning the absolute ages. Finally, (iii) palaeoclimatic implications of the dating results are addressed.

2. ^{10}Be surface exposure dating

The development of surface exposure dating during the last two decades enables the direct determination of deposition ages of boulders and moraines (Cerling and Craig, 1994; Gosse and Phillips, 2001). The method is based on the in-situ production of so-called cosmogenic nuclides (like, e.g. ^{10}Be, ^{26}Al and ^{36}Cl) within the first few decimetres of an exposed rock surface. In quartz, ^{10}Be is mainly produced by spallation reactions of fast neutrons and muons with silica and oxygen. The local production rate of cosmogenic nuclides depends on the intensity of the cosmic radiation. Therefore, both the latitude and the altitude of the sample location must be known for the calculation of the exposure time. The latitude determines the amount of primary cosmic radiation (mainly protons and α-particles) that reaches the upper atmosphere after deflection in the geomagnetic field. A cascade of nuclide reactions in the upper atmosphere produces the secondary cosmic radiation (mainly neutrons and muons), which is then more or less exponentially attenuated on its way to the earth surface. Recently, so-called scaling systems have been developed that do not only allow to calculate local production rates for all geographical positions (the reference production rate refers to sea level and high latitude, SLHL); additionally, these models enable to correct the exposure ages for past changes in the geomagnetic field (Desilets and Zreda, 2003; Dunai, 2001).

The exposure ages in this study were calculated according to Desilets and Zreda (2003), using a reference production rate of 5.25 atoms a^{-1} g^{-1} SiO_2 for neutron spallation. This value has been derived from recalculation of cosmogenic nuclide data of the well-dated Köfels landslide in Austria (Kubik and Ivy-Ochs, 2004; Kubik et al., 1998). All exposure ages were corrected for changes of the magnetic field intensity (and according to Guyodo and Valet, 1996, for the time >10 ka BP; data according to McElhinny and Senanayake, 1982, for the time <10 ka BP). The dipole wobble can be accounted for during the last 10 ka (data according to Ohno and Hamano, 1992). Before that time, a geocentrical axial dipole can be assumed without inducing major errors. Sample-specific corrections were performed for topographic shielding according to Dunne et al. (1999). No correction was calculated for vegetation or snow cover, because vegetation is extremely sparse and the selection of large boulders for sampling can be expected to reduce snow cover effects in the arid research area.

Large granite boulders (e.g. Figs. 3 and 4) were sampled at their top with hammer and chisel (0.5–1 kg). The laboratory procedure was conducted following a slightly modified scheme of Ivy-Ochs (1996): After separation of pure quartz by selective chemical dissolution and addition of a Be carrier, the samples were dissolved in concentrated HF. Anion and cation exchange chromatography were then performed to purify the Beryllium. For the AMS measurements (accelerated mass spectrometer) at the ETH/PSI tandem facility in Zurich, Be-hydroxide was precipitated, baked to the oxide and pressed into targets.

3. Research area—the Encierro Valley

The Encierro Valley (29°05′S, 60°54′W, Figs. 1 and 2) is located just south of the Arid Diagonal. It experiences a steep precipitation gradient with rates of 100 mm/a at 26°S and at 4000 m a.s.l. increasing to 400 mm/a at 30°S and at the same altitude. Precipitation in the Encierro Valley is estimated to 300 mm/a and mainly falls in austral winter (Vuille and Ammann, 1997). Due to the dry conditions, glaciers currently do not exist, although the catchment reaches altitudes above 5000 m. Moraines are found down to 3500 m altitude and document the considerable extent of former glaciations. Previous investigations (Grosjean et al., 1998; Jenny and Kammer, 1996; Veit, 1994) distinguish up to five glacial stages (Fig. 2). Apart from Late Holocene radiocarbon ages (Grosjean et al., 1998), absolute dates from the area are not available so far. Based on correlation with glacial advances to the north, Veit (1994) assigned an age older than 30 ka BP and a late-glacial age to the most extensive moraines (M-I and M-II, respectively, ELA depressions ~1000 m). Recent modelling suggests a precipitation increase of ~550 mm/a and a regional temperature depression of ~5.5 °C compared to today for the prominent glacial stage M-II (Kull et al., 2002). It has been proposed that this palaeoclimate scenario may indicate that the glacial advance M-II occurred during full glacial climate conditions.

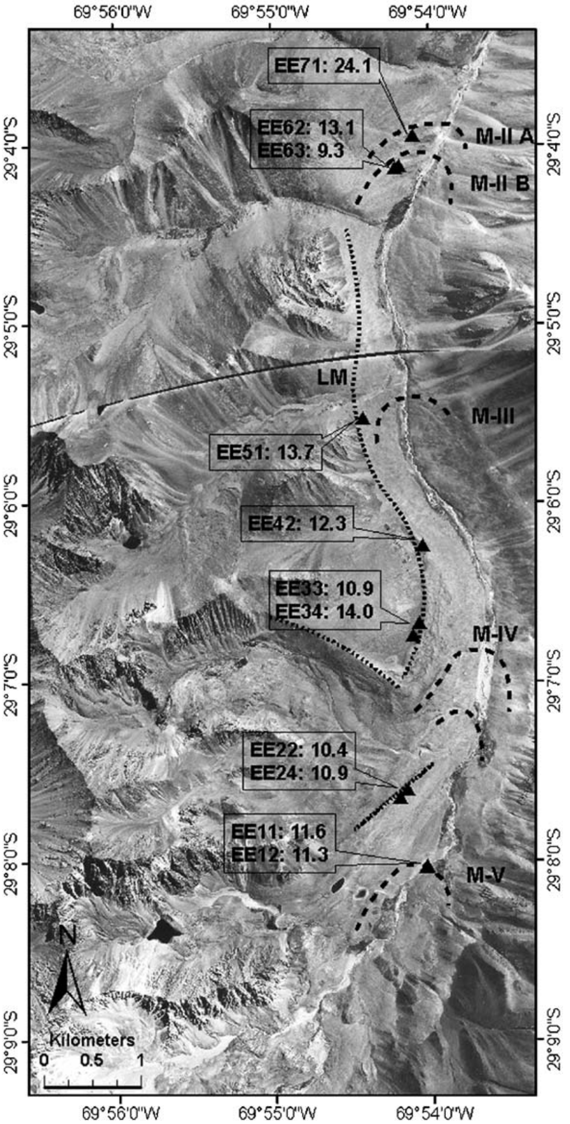

Fig. 2. Geomorphological setting of the sampling locations and exposure ages in ka BP. The dashed lines indicate terminal moraines and the dotted lines pronounced lateral moraines. Labelling of the moraines follows previous stratigraphic work (Grosjean et al., 1998), supplemented by the division of the M-II moraine into M-II A and B, the addition of M-V as a younger recession stage and the huge lateral moraine LM.

Fig. 3. View from the inner terminal moraine arc in northern direction (sampling of boulder EE62). Behind, the outer terminal moraine forms the smooth east-facing slope.

In order to contribute to the reconstruction of the glacial history of the Encierro Valley, 11 large granite boulders from several moraines were selected for ^{10}Be surface exposure dating (Triassic granites crop out in the upper part of the valley according to Nasip et al., 1990). Fig. 2 illustrates the geomorphological setting of the sample sites:

(i) Two boulders (EE11 and 12) on a recessional moraine in the main valley (M-V) were selected for sampling, in order to characterise the deglaciation. Two more boulders (EE22 and 24) were sampled on a lateral moraine to the northwest.
(ii) The large lateral moraine LM reveals a hummocky relief in its upper part, but a crest-shaped

Fig. 4. View from the outer terminal moraine arc (dashed line) in southwestern direction (in the foreground sample EE71). Behind, one can see the transition of the lateral moraine LM to the inner terminal moraine arc (dotted line). The arrow indicates the ice-flow direction.

morphology in the middle and lower parts. All three parts of LM were therefore sampled independently (EE33, EE34, EE42 and EE51).

(iii) Two boulders were sampled from an inner terminal moraine arc (M-II B) at an altitude of 3680 m (EE62 and 63) and, finally, one boulder (EE71) was sampled from the outer terminal moraine arc (M-II A) (see Figs. 3 and 4).

4. Results and discussion

The sample data and calculated exposure ages are given in Table 1 and illustrated in their stratigraphical context in Fig. 2. For the discussion of the exposure ages, we will first concentrate on sample-specific effects, i.e. topographic shielding, sample thickness and geometry, pre-exposure, rock surface erosion and post-depositional geomorphological activity. The potential effects of these factors on the dating results must be understood in order to draw sound conclusions from the sample exposure ages to the deposition ages of the moraines. In a second step, we will discuss systematic uncertainties, i.e. those induced by the reference production rate, the scaling system and potential neotectonic activity. These uncertainties affect all samples in the same way and must be considered when interpreting the exposure ages as 'absolute' ages in the palaeoclimatic context.

4.1. Sample-specific effects—relative glacial chronology

The concentration of accumulated cosmogenic nuclides from boulders on one and the same moraine do not necessarily agree with each other. Occasionally, the data scatter can be much larger than the standard deviations of the AMS measurements. This is also the case for the lateral moraine LM (samples EE33, 34, 42 and 51) and the terminal moraine M-II B (EE62 and 63, see also Fig. 5). Exposure ages may scatter due to different topographic shielding of the cosmic radiation, deviating sample geometries, pre-exposure, rock surface erosion or due to unstable landform surfaces. The correction factors for topographic shielding are less than 1.5% (Table 1). Sample thickness correction, which is the only feasible geometric correction hitherto, might be up to 3% (4 cm sample thickness) assuming an exponential decrease of the isotope concentration with depth (Lal, 1991). This correction was however not applied, because there is no consensus yet (Masarik and Reedy, 1995). Other geometric

Table 1
Sample data and exposure ages calculated according to Desilets and Zreda (2003)

Sample	Latitude °S	Longitude °W	Altitude [m a.s.l.]	^{10}Be [at/g SiO_2]	AMS SD[a] [%]	Topographic shielding	Exposure age[b] [ka BP]
EE11	29.13	69.90	3971	801,054	4.1	0.997	11.6 ± 0.5
EE12	29.13	69.90	3971	783,229	3.7	0.997	11.3 ± 0.4
EE22	29.13	69.90	3998	732,037	3.7	0.997	10.4 ± 0.4
EE24	29.13	69.90	3994	764,244	4.2	0.997	10.9 ± 0.5
EE33	29.11	69.90	4055	791,946	5.9	0.997	10.9 ± 0.7
EE34	29.11	69.90	4029	1,004,234	4.8	0.997	14.0 ± 0.6
EE42	29.10	69.90	3955	838,268	4.3	0.997	12.3 ± 0.5
EE51	29.09	69.90	3900	897,528	4.2	0.984	13.7 ± 0.5
EE62	29.07	69.90	3688	755,000	5.2	0.988	13.1 ± 0.7
EE63	29.07	69.90	3684	530,162	4.1	0.988	9.3 ± 0.4
EE71	29.07	69.90	3678	1,472,753	4.1	0.988	24.1 ± 0.9

[a] AMS SD = 1σ standard deviation of the AMS measurement.
[b] Including the propagated 1σ standard deviation of the AMS measurement.

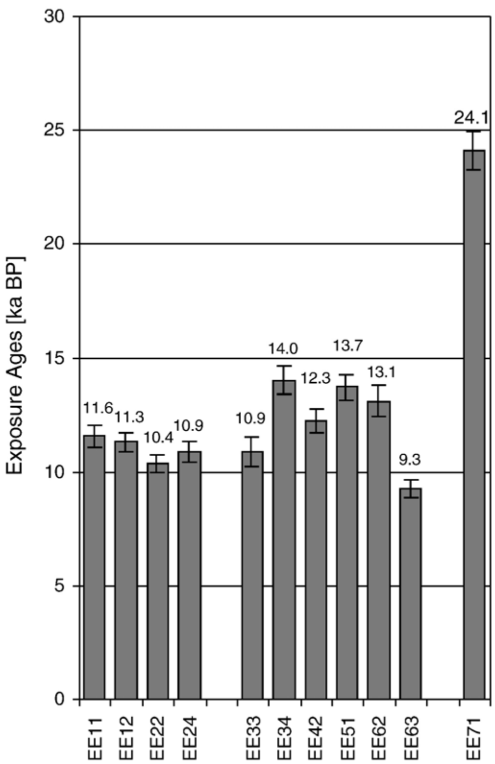

Fig. 5. Sample-specific effects and uncertainties on the exposure ages. The error bars indicate the 1σ standard deviations of the AMS measurements.

effects, like sample height or proximity to boulder edges, should be less than 10% (Masarik and Wieler, 2003).

An explanation for the overestimation of the deposition age of moraines is pre-exposure, also termed inheritance (see Fig. 5). The probability of inheritance is assumed to be as low as <3% (Putkonen and Swanson, 2003; Shanahan and Zreda, 2000). On the other side, underestimation of the deposition age occurs when accumulated cosmogenic nuclides are lost due to rock surface erosion (see Fig. 5). This effect is largest for a sudden and recent erosion event (~10% for a recent loss of the upper 10 cm of the rock surface). Careful sampling, avoiding boulders with signs of erosion and looking for boulders with striae instead, can minimise the risk of unrevealed erosion. The underestimation of the deposition age of a moraine due to unstable landform surfaces is most important in our case study. Formerly buried boulders could be exhumed due to erosion of surrounding soil matrix (Hallet and Putkonen, 1994; Putkonen and Swanson, 2003), or due to upheaval or rotation of boulders during cryoturbation processes. Ice-cored moraines, which can often be recognised from their hummocky relief, remain unstable as long as cold conditions prevent the buried ice from melting. This may take up to thousands of years (Zech et al., 2005). Following this argumentation, the oldest exposure age from a moraine can be considered to be the best estimate for the deposition age, whereas the youngest exposure age should be close to the time of landform surface stabilization. This approach for interpreting exposure ages, known as 'oldest age model', should generally be preferred over calculating mean ages, unless an 'inheritance-boulder' has been identified on the basis of stratigraphic constraints or the exposure age distribution (i.e. an obvious outlier). A huge number of available dates would of course be useful to identify inheritance, but exposure dating is elaborate and expensive.

Based on our 11 exposure ages, we tentatively suggest the following relative chronology:

(i) The samples EE11, 12, 22 and 24 document the deglaciation in the Encierro Valley. Although the exact stratigraphic situation is complicated by the western tributary valleys, the exposure ages clearly date recessional glacial stages. According to the 'oldest age model', the oldest sample, boulder EE11, most likely dates the timing of the last glacial advance. Rapid warming then caused deglaciation and melting of buried glacier ice (approximately dated by the youngest sample, boulder EE22).

(ii) The samples on the lateral moraine LM stratigraphically belong to the most prominent glacial stage, which terminates with M-II B. Similar ages should therefore be expected for LM and M-II B. However, out of six samples, three seem to underestimate the deposition age (EE33, 42 and 63). This is likely due to post-depositional geomorphological instability. Boulder EE33 lies on the hummocky upper part of LM, and boulder EE63 might have been affected by delayed melting of buried glacier ice in an ice-cored terminal moraine. According to the 'oldest age model', sample EE34 can be considered to be the best estimate for the timing of the corresponding glacial advance. The youngest sample, boulder EE63, approximately dates the stabilization of the moraine surface.

(iii) Only one exposure age is available for M-II A (EE71). We tentatively interpret this age as deposition age of a glacial advance that occurred much earlier than the subsequent ones, but this conclusion clearly requires verification in future studies.

4.2. Systematic uncertainties—absolute glacial chronology

Before the exposure ages can be discussed in terms of their absolute values and in the context of the climate history, one should be aware of systematic uncertainties of the dating method. These affect all samples in the same way. Up to now, there exist only very few calibration studies and no reference production rate that has been agreed upon. Furthermore, slightly differing scaling systems are available.

As outlined above, we recalculated a reference production rate from the data of the well-dated Köfels landslide (Kubik and Ivy-Ochs, 2004) and used the scaling system described by Desilets and Zreda (2003). In Fig. 6, the ±10% error bars illustrate the total systematic uncertainties as suggested by Gosse and Phillips (2001). They include the uncertainty of the basic calibration, altitude scaling and geographical scaling. Only local calibration studies could further reduce these uncertainties, because they could take into account persistent anomalies in the atmosphere (affecting altitude scaling) and anomalies in the geomagnetic field (affecting geographical scaling). Local calibration studies are, however, not available for the Central Andes so far. The second column in Fig. 6 illustrates the exposure ages that are obtained when applying the scaling system of Dunai (2001) instead of the one of Desilets and Zreda (2003). No significant difference can be observed. A hypothetical uplift rate of 5 mm/a would not dramatically affect the exposure ages either (third column in Fig. 6).

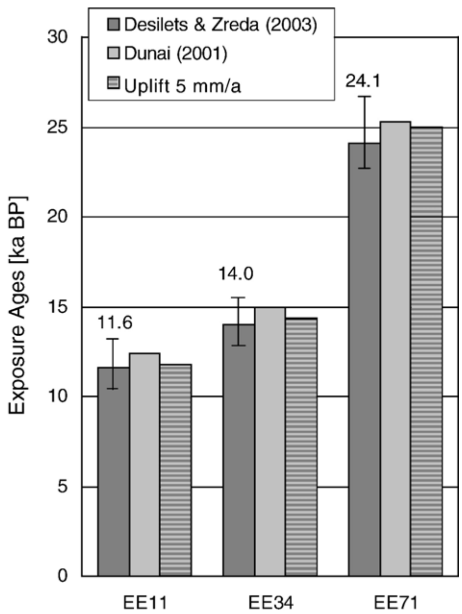

Fig. 6. Systematic uncertainties of the exposure ages. The first and second columns illustrate the age difference between calculations based on the scaling systems of Desilets and Zreda (2003) and of Dunai (2001), respectively. The third column shows the potential influence of an assumed neotectonic uplift. The ±10% error bar represents the total systematic uncertainties (Gosse and Phillips, 2001).

In conclusion, being aware of the potential sample-specific and systematic uncertainty of ±10% (Gosse and Phillips, 2001), we propose the following glacial chronology for the Encierro Valley:

(i) The recessional stage M-V occurred at 11.6 ± 1.2 ka BP (sample EE11).

(ii) The most prominent glacial stage, documented by the large lateral moraine LM and the terminal moraine M-II B, belongs to a late-glacial advance that occurred at 14.0 ± 1.4 ka BP (EE34). Final melting of buried glacier ice and subsequent stabilization of the landform surfaces could be dated into the Early Holocene (EE22: 10.4 ± 1.0 ka BP and EE63: 9.3 ± 0.9 ka BP, respectively).

(iii) Although based on one exposure age only, we tentatively suggest that a slightly more extensive glaciation occurred at 24.1 ± 2.4 ka BP (EE71).

5. Palaeoclimatic context and outlook

Our dates south of the Arid Diagonal suggest increased humidity and related major glacier advances before the LGM at ~25 ka BP, and afterwards at ~14 ka BP. Modelling results from a glacier-climate study indicate a temperature depression of 5.5 °C and a precipitation increase to 550 mm/a for the M-II stages in the Encierro Valley (Kull et al., 2002). Today, the study area is mainly influenced by the westerlies and winter precipitation.

Based on the rise of (palaeo) ELAs and the lack of present glaciers towards the Centre of the Arid Diagonal, it has been argued that the areas north and south of the Arid Diagonal are and were mainly influenced by different climatic systems—by the westerlies in the south (from 27° southward) and by tropical summer precipitation in the north (from 24° northward). However, a not negligible amount of summer precipitation in the Encierro Valley originates from the advection of humid air masses from the Andean east-side and might have played an important role during the observed glacial stages.

Whereas the glacier-climate model could not determine the seasonality of the precipitation in the study area, modelling results from the western Cordillera at 18°S and 23°S indicate very wet past climate conditions, which are clearly related to increased late-glacial summer precipitation (Kull, 1999; Kull and Grosjean, 2000). The temperature depression there was calculated to only 2–3 °C, which is less than the temperature depression of 5.5 °C in the Encierro Valley. The exact timing of the modelled glacial advances north of the Arid Diagonal awaits further exposure age analysis.

Although a detailed surface exposure age chronology from the Bolivian Altiplano is not yet available either, the glacial chronology in the Encierro Valley may indicate some similarities in the glacial history: Clapperton et al. (1997) had proposed glacial phases for 34–27 ka BP (Choqueyapu I), 14–13 ka BP (Choqueyapu II) and 12–10 ka BP on the eastern Altiplano. They correlated the glacial phases with periods of high lake levels, implying that moisture advection to the Central Andes is an important trigger for glacial advances. Logging data from the Salar de Uyuni, Bolivia, corroborate this view. Lacustrine muds were deposited from 25 ka BP to the late glacial, with peaks around 25, 15 and 12 ka BP (Baker et al., 2001). The $\delta^{18}O$ values from the Sajama ice core in Bolivia (Thompson et al., 1998) can also be interpreted as precipitation proxy (Ramirez et al., 2003), indicating wetter conditions until 15 ka BP and again from 14 to 12 ka BP. The conclusions that can be drawn from these proxies are, however, ambiguous. Smaller hydrological catchments and lakes on the southern Altiplano, for instance, indicate dry conditions during the LGM (Grosjean et al., 2001), so that the influence of the monsoon on the Altiplano remains speculative.

The general view–that the areas south of the Arid Diagonal are and were mainly influenced by the westerlies–may underestimate the complex and in space and time variable interaction between the westerlies and the tropical summer precipitation regime. Pollen analyses around 25°S indicate, for example, increased precipitation in both seasons between 17 and 14 ka BP, but more winter precipitation before and more summer precipitation thereafter (Maldonado et al., 2005). It is the goal of ongoing research to date further glacial stages north and south of the Arid Diagonal in order to establish more precise glacial chronologies and to identify changes in the atmospheric circulation pattern.

Acknowledgement

This study was made possible by funding through the Swiss National Science Foundation (SNF project 21-067937.02/1) and the 'Studienstiftung des deutschen Volkes e.V.'. We also thank M. Grosjean and M. Vuille for constructive discussions.

References

Ammann, C., Jenny, B., Kammer, K., Messerli, B., 2001. Late Quaternary glacier response to humidity changes in the arid Andes of Chile (18–29°S). Palaeogeography, Palaeoclimatology, Palaeoecology 172, 313–326.

Baker, P.A., Rigsby, C.A., Seltzer, G.O., Fritz, S.C., Lowenstein, T.K., Bacher, N.P., Veliz, C., 2001. Tropical climate changes at millennial and orbital timescales on the Bolivian Altiplano. Nature 409, 698–701.

Caviedes, C.N., 1990. Rainfall variation, snowline depression and vegetational shifts in Chile during the Pleistocene. Climatic Change 16, 99–114.

Cerling, T.E., Craig, H., 1994. Geomorphology and in-situ cosmogenic isotopes. Annual Reviews of Earth and Planetary Sciences 22, 273–317.

Chepstow-Lusty, A., Bush, M.B., Frogley, M.R., Baker, P.A., Fritz, S.C., Aronson, J., 2005. Vegetation and climate change on the Bolivian Altiplano between 108,000 and 18,000 yr ago. Quaternary Research 63, 90–98.

Clapperton, C.M., Clayton, J.D., Benn, D.I., Marden, C.J., Argollo, J., 1997. Late Quaternary glacier advances and palaeolake highstands in the Bolivian Altiplano. Quaternary International 38–39, 49–59.

Clayton, J.D., Clapperton, C.M., 1997. Broad synchrony of a late-glacial glacier advance and the highstand of palaeolake Tauca in the Bolivian Altiplano. Journal of Quaternary Science 12, 169–182.

Denton, G.H., Lowell, T.V., Heusser, C.J., Schlüchter, C., Andersen, B.G., Heusser, L.E., Moreno, P.I., Marchant, D.R., 1999. Geomorphology, stratigraphy, and radiocarbon chronology of Llanquihue drift in the area of the southern Lake District, Seno Reloncavi, and Isla Grande de Chiloe, Chile. Geografiska Annaler 81(A), 167–229.

Desilets, D., Zreda, M., 2003. Spatial and temporal distribution of secondary cosmic-ray nucleon intensities and applications to in situ cosmogenic dating. Earth and Planetary Science Letters 206, 21–42.

Dunai, T.J., 2001. Influence of secular variation of the geomagnetic field on production rates of in situ produced cosmogenic nuclides. Earth and Planetary Science Letters 193, 197–212.

Dunne, A., Elmore, D., Muzikar, P., 1999. Scaling factors for the rates of production of cosmogenic nuclides for geometric shielding and attenuation at depth on sloped surfaces. Geomorphology 27, 3–11.

Espizua, L.E., 1999. Chronology of Late Pleistocene glacier advances in the Rio Mendoza Valley, Argentina. Global and Planetary Change 22, 193–200.

Fritz, S.C., Baker, P.A., Lowenstein, T.K., Seltzer, G.O., Rigsby, C.A., Dwyer, G.S., Tapia, P.M., Arnold, K.K., Ku, T., Luo, S., 2004. Hydrologic variation during the last 170,000 years in the southern hemisphere tropics of South America. Quaternary Research 61, 95–104.

Garleff, K., Stingl, H. (Eds.), Südamerika: Geomorphologie und Paläoökologie im jüngeren Quartär, Bamberger Geographische Schriften, vol. 11. 394 pp.

Garleff, K., Stingl, H. (Eds.), 1998. Landschaftsentwicklung, Paläoökologie und Klimageschichte der Ariden Diagonale Südamerikas im Jungquartär, Bamberger Geographische Schriften, vol. 15. 401 pp.

Geyh, M.A., Grosjean, M., Nunez, L., Schotterer, U., 1999. Radiocarbon effect and the timing of the late-glacial/Early Holocene humid phase in the Atacama desert (northern Chile). Quaternary Research 52, 143–153.

Gosse, J.C., Phillips, F.M., 2001. Terrestrial in situ cosmogenic nuclides: theory and application. Quaternary Science Reviews 20, 1475–1560.

Grosjean, M., Geyh, M., Messerli, B., Schotterer, U., 1995. Late-glacial and Early Holocene lake sediments, groundwater formation and climate in the Atacama Altiplano. Journal of Paleolimnology 14, 241–252.

Grosjean, M., Geyh, M.A., Messerli, B., Schreier, H., Veit, H., 1998. A Late-Holocene (<2600 BP) glacial advance in the south-central Andes (29°S), northern Chile. The Holocene 8 (4), 473–479.

Grosjean, M., van Leeuwen, J.F.N., van der Knaap, W.O., Geyh, M.A., Ammann, B., Tanner, W., Messerli, B., Veit, H., 2001. A 22,000 ^{14}C yr BP sediment and pollen record of climate change from Laguna Miscanti (23°S), northern Chile. Global and Planetary Change 28, 35–51.

Guyodo, Y., Valet, J.-P., 1996. Relative variations in geomagnetic intensity from sedimentary records: the past 200,000 years. Earth and Planetary Science Letters 143, 23–26.

Hallet, B., Putkonen, J., 1994. Surface dating of dynamic landforms: young boulders on aging moraines. Science 265, 937–940.

Harrison, S.P., 2004. The Pleistocene glaciations of Chile. In: Ehlers, J., Gibbard, P.L. (Eds.), Quaternary Glaciations—Extent and Chronology: Part III. South America, Asia, Africa, Australasia, Antarctica. Elsevier, Cambridge.

Hastenrath, S., Kutzbach, J., 1985. Late Pleistocene climate and water budget of the south American Altiplano. Quaternary Research 24, 249–256.

Heine, K., 2004. Late Quaternary glaciations of Bolivia. In: Ehlers, J., Gibbard, P.L. (Eds.), Quaternary Glaciations—Extent and Chronology: Part III. South America, Asia, Africa, Australasia, Antarctica. Elsevier, Cambridge.

Heusser, C.J., Heusser, L., Lowell, T.V., 1999. Paleoecology of the southern Chilean lake district–Isla Grande de Chiloé during middle–late Llanquihue glaciation and deglaciation. Geografisca Annaler 81, 231–284.

IPCC, 2001. Third Assessment Report. www.ipcc.ch.

Ivy-Ochs, S., 1996. The dating of rock surface using in situ produced ^{10}Be, ^{26}Al and ^{36}Cl, with examples from Antarctica and the Swiss Alps. Diss. ETH No. 11763, Zürich. 197 pp.

Jenny, B., Kammer, K., 1996. Jungquartäre Vergletscherung. In: Ammann, C., Jenny, B., Kammer, K. (Eds.), Climate Change in den Trockenen Anden, Geographica Bernensia, vol. G46, pp. 1–80.

Kubik, P., Ivy-Ochs, S., 2004. A re-evaluation of the 0–10 ka ^{10}Be production rate for exposure dating obtained from the Köfels (Austria) landslide. Nuclear Instruments and Methods in Physics Research B 223–224, 618–622.

Kubik, P.W., Ivy-Ochs, S., Masarik, J., Frank, M., Schlüchter, C., 1998. ^{10}Be and ^{26}Al production rates deduced from an instantaneous event within the dendro-calibration curve, the landslide of Köfels, Ötz Valley, Austria. Earth and Planetary Science Letters 161, 231–241.

Kull, C., 1999. Modellierung paläoklimatischer Verhältnisse basierend auf der jungpleistozänen Vergletscherung in Nordchile-Ein Fallbeispiel aus den Nordchilenische Anden. Zeitschrift für Gletscherkunde und Glazialgeologie 35, 35–64.

Kull, C., Grosjean, M., 1998. Albedo changes, Milankovitch forcing, and lake quaternary climate changes in the central Andes. Climate Dynamics 14, 871–881.

Kull, C., Grosjean, M., 2000. Late Pleistocene climate conditions in the north Chilean Andes drawn from a climate-glacier model. Journal of Glaciology 46, 622–632.

Kull, C., Grosjean, M., Veit, H., 2002. Modeling modern and Late Pleistocene glacio-climatological conditions in the North Chilean Andes (29–30°). Climatic Change 52, 359–381.

Kull, C., Hanni, F., Grosjean, M., Veit, H., 2003. Evidence of an LGM cooling in NW-Argentina (22°S) derived from a glacier climate model. Quaternary International 108 (1), 3–11.

Lal, D., 1991. Cosmic ray labelling of erosion surfaces: in situ nuclide production rates and erosion models. Earth and Planetary Science Letters 104, 429–439.

Lowell, T.V., Heusser, C.J., Andersen, B.G., Moreno, P.I., Hauser, A., Heusser, L.E., Schlüchter, C., Marchant, D.R., Denton, G.H., 1995. Interhemispheric correlations of Late Pleistocene glacial events. Science 269, 1541–1549.

Maldonado, A., Betancourt, J.L., Latorre, C., Villagran, C., 2005. Pollen analysis from a 50,000-yr rodent midden series in the southern Atacama desert (25°30′S). Journal of Quaternary Science 20 (5), 493–507.

Mark, B.G., Seltzer, G.O., Rodbell, D.T., 2004. Late Quaternary glaciations of Ecuador, Peru and Bolivia. In: Ehlers, J., Gibbard, P.L. (Eds.), Quaternary Glaciations—Extent and Chronology: Part III. South America, Asia, Africa, Australasia, Antarctica. Elsevier, Cambridge.

Masarik, J., Reedy, R.C., 1995. Terrestrial cosmogenic-nuclide production systematics calculated from numerical simulations. Earth and Planetary Science Letters 136, 381–395.

Masarik, J., Wieler, R., 2003. Production rates of cosmogenic nuclides in boulders. Earth and Planetary Science Letters 216, 201–208.

McElhinny, M.W., Senanayake, W.E., 1982. Variations in the geomagnetic dipole 1: the past 50,000 years. Journal of Geomagnetism and Geoelectricity 34, 39–51.

Messerli, B., 1973. Problems of vertical and horizontal arrangement in the high mountains of the extreme arid zone (Central Sahara). Arctic and Alpine Research 5(A), 139–147.

Nasip, C., Moscoso, R., Maksaev, V., 1990. Hoja Guanta, Carta Geologica de Chile 1:250 000. Boletin-Servicio Nacional de Geologia y Mineria 67, 1–140.

Ohno, M., Hamano, Y., 1992. Geomagnetic poles over the past 10,000 years. Geophysical Research Letters 19, 1715–1718.

Putkonen, J., Swanson, T., 2003. Accuracy of cosmogenic ages for moraines. Quaternary Research 59, 255–261.

Ramirez, E., Hoffmann, G., Taupin, J.D., Francou, B., Ribstein, P., Caillon, N., Ferron, F.A., Landais, A., Petit, J.R., Pouyaud, B., Schotterer, U., Simoes, J.C., Stievenard, M., 2003. A new Andean deep ice core from the Nevado Illimani (6350 m), Bolivia. Earth and Planetary Science Letters 212, 337–350.

Shanahan, T.M., Zreda, M., 2000. Chronology of quaternary glaciations in East Africa. Earth and Planetary Science Letters 177, 23–42.

Stuut, J.-B.W., Lamy, F., 2004. Climate variability at the southern boundaries of the Namib (south-western Africa) and Atacama

(northern Chile) coastal deserts during the last 120,000 yr. Quaternary Research 62 (3), 301–309.
Sylvestre, F., Servant, M., Servant-Vildary, S., Causse, C., Fournier, M., Ybert, J.-P., 1999. Lake-level chronology on the southern Bolivian Altiplano (18–23 S) during late-glacial time and the Early Holocene. Quaternary Research 51, 54–66.
Thompson, L.G., Davis, M.E., Mosley-Thompson, E., Sowers, T.A., Henders on, K.A., Zagorodnov, V.S., Lin, P.-N., Mikhalenko, V.N., Campen, R.K., Bolzan, J.F., Cole-Dai, J., Francou, B., 1998. A 25,000-year tropical climate history from Bolivian ice cores. Science 282, 1858–1864.
Veit, H., 1994. Jungquartäre Landschafts-und Klimaentwicklung am Südrand der Atacama (Norte Chico, Chile). Universität Bayreuth. Habil. Thesis.
Veit, H., 2000. Klima-und Landschaftswandel in der Atacama. Geographische Rundschau 52 (9), 4–9.
Vuille, M., Ammann, C., 1997. Regional snowfall patterns in the high, arid Andes (South America). Climatic Change 36, 413–423.
Wyrwoll, K.-H., Dong, B., Valdes, P., 2000. On the position of southern hemisphere westerlies at the last glacial maximum: an outline of AGCM simulation results and evaluation of their implications. Quaternary Science Reviews 19, 881–898.
Zech, R., Glaser, B., Sosin, P., Kubik, P.W., Zech, W., 2005. Evidence for long-lasting landform surface instability on hummocky moraines in the Pamir Mountains from surface exposure dating. Earth and Planetary Science Letters 237 (3–4), 453–461.